



A GENUINELY MULTIDISCIPLINARY JOURNAL

CHEMPLUSCHEM

CENTERING ON CHEMISTRY

Accepted Article

Title: Optoelectronic Properties of A- π -D- π -A Thiophene-Based Materials with a Dithienosilole Core: An Experimental and Theoretical Study

Authors: Francesca Parenti, Monica Caselli, Davide Vanossi, Mirko Buffagni, Manuel Imperato, Laura Pigani, and Adele Mucci

This manuscript has been accepted after peer review and appears as an Accepted Article online prior to editing, proofing, and formal publication of the final Version of Record (VoR). This work is currently citable by using the Digital Object Identifier (DOI) given below. The VoR will be published online in Early View as soon as possible and may be different to this Accepted Article as a result of editing. Readers should obtain the VoR from the journal website shown below when it is published to ensure accuracy of information. The authors are responsible for the content of this Accepted Article.

To be cited as: *ChemPlusChem* 10.1002/cplu.201900092

Link to VoR: <http://dx.doi.org/10.1002/cplu.201900092>

WILEY-VCH

www.chempluschem.org

A Journal of



Optoelectronic Properties of A- -D- -A Thiophene-Based Materials with a Dithienosilole Core: An Experimental and Theoretical Study

Monica Caselli^[a], Davide Vanossi^[a], Mirko Buffagni^[a], Manuel Imperato^[a], Laura Pigani^[a], Adele Mucci^[a], Francesca Parenti^{*[a]}

^[a] Dr. M. Caselli, Dr. D. Vanossi, Dr. M. Buffagni, Dr. M. Imperato, Dr. L. Pigani, Prof. A. Mucci, Dr. F. Parenti, Dipartimento di Scienze Chimiche e Geologiche, Università di Modena e Reggio Emilia, Via G. Campi 103, 41125 Modena, Italy

E-mail: francesca.parenti@unimore.it

Supporting Information is available

Abstract: Two A- -D- -A thiophene based small molecules, with a central dithienosilole core and dicyanovinyl end groups were synthesized. These compounds differ only for the presence of alkyl and alkylsulfanyl chains, respectively, on thiophene beta positions. The computational data together with the spectroscopic and electrochemical findings (obtained by means of absorption, steady-state/time-resolved emission techniques and cyclic voltammetry) revealed that both molecules possess low electronic and optical band gaps, broad absorption spectra and a good stability both in p and n-doping states, properties that make them suitable for optoelectronic applications. In either compounds the HOMO-LUMO transition involves an intramolecular charge transfer from the electron-donor dithienosilole unit to the two terminal electron-acceptor DCV groups. A marked positive emission solvatochromism was observed for both molecules and was interpreted on the basis of the symmetry breaking in the S₁ excited state. The two synthesized compounds were also compared to their shorter precursors and to similar oligothiophenes to understand how the nature of the building block influences the characteristics of the final materials. Furthermore, it was possible to better understand the contribution of the sulfur atom in modulating the optical properties of the small molecules studied.

Introduction

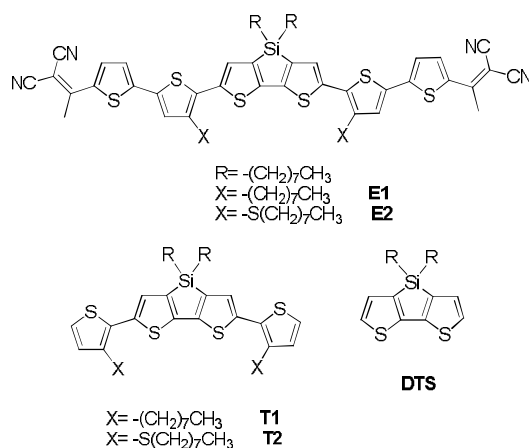
Organic electronics is mainly based on conducting polymers, widely studied functional materials which find applications in organic solar cells (OSC), organic light emitting diodes (OLED), organic field-effect transistors (OFET), fluorescence sensors and biosensors.^[1-4] The versatility of these polymers is due to their stability and to the uniqueness of their electronic and optical features. Conductive polymers are obtained by relatively simple synthetic protocols, which make a fine-tuning of their properties possible, in view of modulating and improving the performance of the final devices. The principal drawback is that, like all polymers, they suffer from lack of synthetic reproducibility. Conjugated oligomers possess similar or even better electronic properties, e.g. often exhibit higher charge mobility and polarizability and, in addition, are structurally well-defined, monodisperse, free of structural defects. Moreover, oligomers are prone to form ordered supramolecular structures and this has recently shown to have significant repercussions on the performance of the final device.^[5,6] In particular, small conjugated molecules such as oligothiophenes (OTs), beyond retaining some of the typical molecular characteristics of their homologous with higher molecular weight, have proved to be good materials for OSCs,^[7] OLEDs^[8] and OFETs.^[9-11] The optoelectronic properties of oligothiophenes and, generally, of aromatic π -conjugated systems, are largely a result of the degree of conjugation. The conjugation length and, hence, the optical band gap in solution are influenced by four variables: aromatic or quinoid character, bond length alternation, torsions along the polymer backbone and electronic effects from side groups.^[12] Among small molecules, the push-pull ones are attracting increasing attention. They are characterized by a widely delocalized π -electron system, resulting in low-energy absorption bands that make them excellent light harvesting systems in optoelectronic devices. Different building blocks of electron donors (D) and acceptors (A), linked through a π -bridge, may be variously combined (i.e. A- π -A, D- π -D, A- π -D, A- π -D- π -A, D- π -A- π -D) and the choice of the donor and acceptor groups makes possible a fine tuning of their electronic band gap. Furthermore, A- π -D- π -A and D- π -A- π -D quadrupolar molecular systems have been studied in relation to their nonlinear optical properties, which make them usable in bio-imaging applications and photodynamic therapy.^[13] Dipolar and quadrupolar molecules undergo intramolecular charge transfer transitions, so their photophysics is dominated by a strong dependence on the nature of the solvent.^[14] Since quadrupolar molecular systems do not possess a permanent electric dipole moment, due to their symmetry, such common observations have been interpreted on the basis of a breaking of the symmetry upon excitation assisted by the solvent.^[15]

Recently A- π -D- π -A thiophene-based small molecules, where the A moiety is a dicyanovinyl group (DCV), have been studied.^[16-20] These molecules, where the backbone has a hole-transporting function whereas the DCV acceptor moiety expands the absorption spectrum to higher wavelengths, should lead to efficient intramolecular charge-transfer and make possible a fine-tuning of the band gap. Moreover, DCV is planar and

contributes to π -stacks formation and strong intermolecular interactions. Among the D units, dithienosilole is intriguing since it possesses rigidity and planarity, reinforced by the interaction between the σ^* orbital of silicon and π^* orbital of bithiophene, stability under ambient conditions and a lower band gap if compared to the carbon analogues.^[21] Several examples that combine the properties of DCV donor and dithienosilole acceptor units are present in the literature.^[22, 24] In particular, methyl-DCV derivatives, where the vinyl hydrogen of the DCV is substituted by a methyl group, seem to be very photostable and to possess good photovoltaic performances.^[25,26]

We have been involved in the synthesis and characterization of poly(alkylsulfanylthiophenes) for several years^[27-30]. For this type of polymers, it has been demonstrated that the electron-donating sulfur atom of the alkylsulfanyl chain causes a red-shift in the absorption spectra and affects both LUMO and HOMO energy levels.^[31,32] In this respect, we are still interested in studying the influence of alkylsulfanyl substituents on the electronic properties of thiophene-based small molecules.

In this paper, we present the synthesis and a combined theoretical and experimental study of the optical, photophysical and electrochemical behavior of two A- π -D- π -A thiophene-based small molecules with a central dithienosilole unit (Scheme 1). The latter is symmetrically bonded to an octyl (**E1**) and an octylsulfanyl (**E2**) bithienyl unit, which in turn is connected to a methyl-DCV group. Their relevant synthetic precursors, **DTS**, **T1** and **T2** (Scheme 1) were also investigated, focusing on the progressive change of the electrochemical, optical and photophysical properties, by means of cyclic voltammetry (CV), absorption and steady-state/time-resolved emission techniques. A marked positive fluorescence solvatochromism was observed only for the quadrupolar-like compounds (**E1** and **E2**), interpreted on the basis of a symmetry-breaking in the S_1 excited state. These observations allow the influence of the nature of building blocks and of substituents on the optical and photophysical properties to be rationalized, and further insights into the design of materials for applications in optoelectronic devices to be gained.

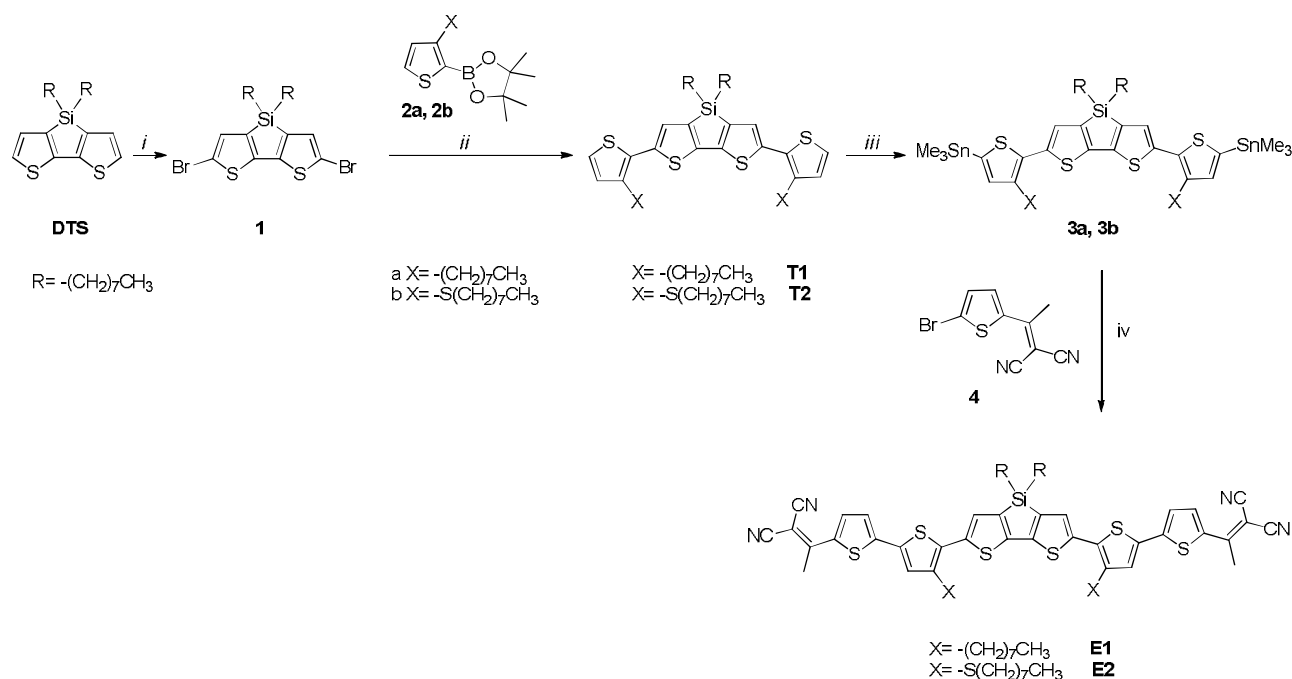


Scheme 1 The A- π -D- π -A thiophene-based small molecules **E1** and **E2** and their building blocks (**T1**, **T2** and **DTS**)

Results and discussion

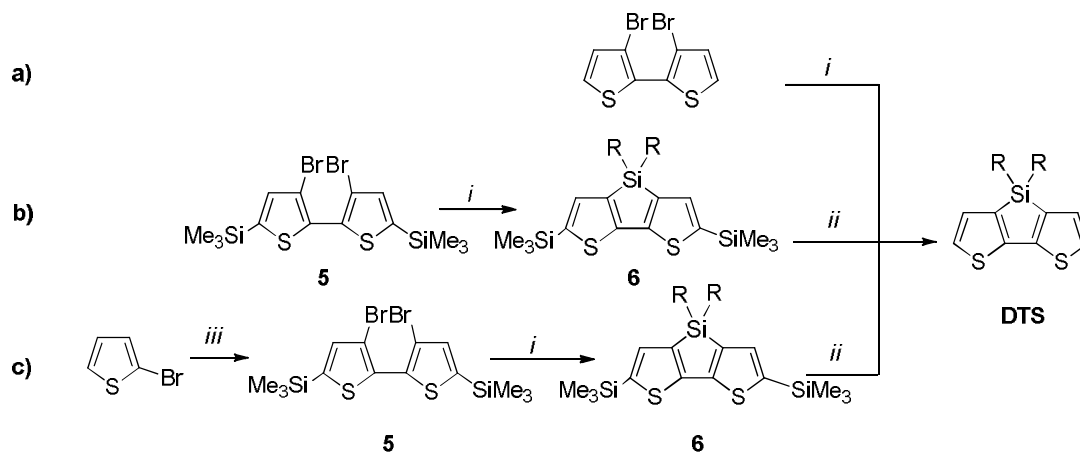
Synthesis

One of the key motifs of **E1** and **E2** here studied is the dithienosilole unit, to which thienyl and thienyl-DCV units are bound in subsequent steps (Scheme 2).



Scheme 2 Synthesis of **E1**, **E2** and the precursors **DTS**, **T1** and **T2**: *i*) NBS; *ii*) Pd(PPh₃)₄, Na₂CO₃; *iii*) LDA, trimethyltin chloride; *iv*) HMDS, acetic acid, malononitrile.

The synthesis of **DTS** can be accomplished starting from 3,3-dibromo-2,2-bithiophene (Scheme 3, route a)^[33, 35] or from 3,3-dibromo-5,5-bis(trimethylsilyl)-2,2-bithiophene (Scheme 3, route b).^[36] Both routes were explored by us and, eventually, we preferred route b with some synthetic modifications (Scheme 3, route c): starting from 2-bromothiophene, the bithiophene **5** was generated by a one-pot reaction^[37], instead of the more cumbersome method usually employed.^[38, 39] The one-pot procedure allows the insertion of the protecting trimethylsilyl groups, the halogen dance of bromine from thiophene to bithiophene positions and the copper-catalyzed coupling of 4-bromo-2-(trimethylsilyl)thiophene without the need of isolating the intermediates. The silole ring closure was achieved in good yield with minor modifications to the procedure reported.^[36] The ¹H NMR spectra of the raw material obtained showed both the presence of **5**, **6** (bis(trimethylsilyl) protected **DTS** **6**) and of its desilylated derivatives. Therefore, we decided to treat the crude with TFA in order to remove all the trimethylsilyl groups, obtaining **DTS** (24 %, overall yield after chromatography). **DTS** was then brominated^[32] to afford **1** (Scheme 2).



Scheme 3 Synthetic pathways for **DTS**: *i*) *n*-butyllithium, dioctyldichlorosilane; *ii*) trifluoroacetic acid; *iii*) LDA, trimethylsilylchloride, then LDA, anhydrous CuCl₂.

Compound **1** was then reacted with dioxaborolanes **2a,b** to generate dithienyl DTSS **T1** and **T2** (Scheme 2). Dioxaborolanes were, in turn, obtained by lithiation and subsequent treatment with 2-isopropoxy-4,4,5,5-tetramethyl-1,3,2-dioxaborolane of 2-bromo-3-octylthiophene or 2-bromo-3-(octylsulfanyl)thiophene. Compounds **T1** and **T2** were reacted with LDA and trimethyltin chloride to generate trimethyltin derivatives **3a,b** which were, eventually, coupled with thienyl-substituted malononitrile **4** to generate **E1** and **E2**. For the synthesis of compound **4** we followed the methods described in the literature for the corresponding aldehyde using piperidine^[41], beta-alanine^[42] or triethylamine^[43] as the base in the Knoevenagel reaction with malononitrile, but unfortunately no product was obtained. 1D and 2D-NMR spectra of the crudes showed signals attributable to the formation of cyclization side-products (Scheme S1). We suppose that these products are formed after deprotonation of the acidic methyl protons of the methyl-DCV group and subsequent nucleophilic attack of the carbanion both on the vinylic carbon of **4** and on the carbonyl group of 2-acetyl-5-bromothiophene. The formation of these byproducts was avoided by using hexamethyldisilazane in acetic acid as the base, following the procedure reported for different substrates^[44] to selectively deprotonate the malononitrile in the Knoevenagel step. Compound **4**, here synthesized for the first time, is an interesting building block for the synthesis of push-pull small molecules bearing methyl-DCV functionalised thiophene as acceptor units. In fact, by taking advantage of the bromine atom of **4**, it is possible to insert this unit directly on different substrates (e.g. using a Stille coupling with a tin derivative) avoiding the use of protecting/deprotecting steps for the carbonyl moiety, which is usually converted into the methyl-DCV group, through a Knoevenagel reaction, at the end of the synthetic route.

Optical and photophysical properties

The absorption and fluorescence spectra of **DTS**, **T1**, **T2**, **E1**, **E2** in *n*-hexane are reported in Figure 1. Similarly to unsubstituted oligothiophenes, **DTS**, **T1** and **T2** absorption and emission features are independent of the solvent polarity. The maximum of the lowest-energy absorption band of **DTS** is at 336 nm in *n*-hexane and acetonitrile, red-shifted with respect to those of 2,2'-bithiophene (maximum at 304 nm). This is consistent with the suggestion that the silicon bridge between the two thiophene rings extends the π -conjugation thanks to the planar structure assumed by the central, three-ring core. Also, silicon gives an appreciable contribution to the LUMO, as shown in Figure S1 in SI, suggesting a hyperconjugative effect able to reduce the optical band gap: such a finding is in agreement with the observed red-shifted absorption spectrum of a dithienosilole derivative with respect to the correspondent compound where Si is substituted by C (323 nm).^[45, 46] The lowest-energy absorption band of **T1**, which bears two β -octylthiophenes in the 2,6 positions of the **DTS** central core, is characterized by a maximum at 403 nm: it is red-shifted with respect to **DTS**, consistently with the fact that the substitution by the thiophene units extends the π -conjugation system (see calculated Kohn-Sham molecular orbitals, KS MO, Figure S1). Furthermore, it is also red-shifted with respect to the unsubstituted quaterthiophene, which shows a maximum at 392 nm^[47], and markedly red-shifted with respect to 3,3'-bis(dimethyl) and 3,3'-bis(octyl)quaterthiophenes (maxima at 383 and 372 nm respectively).^[48, 49] It has been reported that the planarity of OTs, and hence the degree of conjugation, increases as a function of the number of thiophene units; however, insertion of alkyl substituents induces out-of-plane distortions which results in a reduced degree of conjugation and in blue-shifted absorption spectra. Combined quantum-chemical and spectroscopic studies have shown that at room temperature methyl-substituted OTs are characterized by a distribution of torsional conformations in the electronic ground state, resulting in broad absorption spectra with maxima depending on the number and position of the substituents.^[48] The octyl substituents, because of their sterical hindrance, induce an increased departure from planarity of the conjugated backbone, if compared with the methyl ones.^[49] Nonetheless, **T1** and **T2**, which bear octyl or octylsulfanyl substituents on a β -position of the outer thienyl rings, are characterized in apolar solvents by absorption maxima at 403 and 434 nm, respectively: these results can be explained by the role of the planar **DTS** central core which confers a higher degree of conjugation, if compared to dioctyl-substituted quaterthiophenes, thanks to the lack of torsional freedom for the central thiophene units in the ground state. **T2** shows a further red-shifted absorption spectrum with respect to **T1**, also attributable to the sulfur contribution to π -delocalization. Another contribution to the bathochromic shift could derive by the lower distortion in **T2** with respect to **T1** suggested by the stronger deshielding of H-3 NMR signal on the dithienosilole unit going from **DTS** to **T2**. This lower distortion causes H-3 to move closer to the plane of the adjacent thienyl ring in **T2** with respect to **T1** and is in agreement with

previous observations on polythiophenes.^[50] The molar absorption coefficients enhance going from **DTS** to **T1/T2** and to **E1/E2**. This trend is expected on the basis of the increased conjugation length.

In Figure S1 the relevant frontier KS MOs are reported for all the molecules studied. Because the photophysics of these compounds is fully determined by the lowest-lying excited states, we will not dwell on a detailed analysis of the experimental higher-energy absorption bands and computed transition energies. A comparison of the HOMO and LUMO for **T1**, **T2**, **E1** and **E2** indicates the typical increased bond order of the interring bonds upon photoexcitation in OTs. The TDDFT calculated gas-phase one-photon absorption spectra reported in Table S2 show that for all compounds the lowest-energy absorption band is mainly attributable to the HOMO-LUMO transition. The maxima calculated by means of the functional CAM-B3LYP (Table 1) are in rather good agreement with the experimental ones (Table 2). An increase of the S_1 oscillator strengths on passing from **DTS** to **T1/T2** and then to **E1/E2** is also shown in Table S2 and is in agreement with the increase of the experimental molar absorption coefficients. The low charge-transfer character exhibited by the HOMO-LUMO transition is consistent with the lack of absorption solvatochromism for all the studied compounds.

Table 1: KS gap (E_g^{KS}) and optical band gap (E_{gap}) obtained at DFT/LR-TDDFT level.

Molecule	E_g^{KS} /eV		E_{gap} /eV ^[a]		E_{gap} /nm	
	B3LYP	CAM-B3LYP	B3LYP	CAM-B3LYP	B3LYP	CAM-B3LYP
DTS	4.045	6.538	3.681	3.873	337	320
T1	2.944	5.165	2.709	2.998	458	414
T2	2.876	5.089	2.622	2.917	473	425
E1	2.036	4.050	1.827	2.323	679	534
E2	1.853	3.846	1.661	2.208	746	562

^[a]These E_{gap} corresponds to the $S_0 - S_1$ transition energies reported in Table S2.

While **DTS** is characterized by structureless spectra both in absorption and emission, the fluorescence spectra of **T1**, **T2**, **E1** and **E2** in *n*-hexane (Figure 1b) show the typical features of OTs, namely they are structured and narrow, if compared with the correspondent absorption spectra. Such behavior of OTs has been interpreted assuming that a broad potential energy torsional surface in S_0 makes accessible a rather large number of conformations whereas, after photoexcitation in S_1 , OTs relax to a quinoid-type planar conformation characterized by an increased interring bond order. Thus, the torsional potential energy curve is narrower in comparison with the ground-state potential, resulting in a distribution of conformations very close to a planar geometry and in narrower fluorescence spectra.^[51, 52] The vibronic structure in emission spectra of OTs is attributed to vibrational modes efficiently coupled to the electronic transition.^[53]

A marked difference between **DTS**, on one hand, and **T1** and **T2**, on the other, can be observed also in the photophysical behavior (Table 2).

DTS shows a very high fluorescence quantum yield in all solvents and a large Stokes shift, properties which make it suitable as a fluorescent label and a good excitation energy donor for blue-emitting acceptors. The photophysical behavior of **DTS** is markedly different from that of 2,2'-bithiophene: the high fluorescence quantum yield (0.86 in *n*-hexane) and long fluorescence lifetime (7.75 ns) indicate a main radiative deactivation path in **DTS** ($k_F=1.1 \times 10^8 \text{ s}^{-1}$), whereas in 2,2'-bithiophene the excited state deactivation is dominated by intersystem crossing (triplet quantum yield in benzene is 0.99).^[47] **T1**, characterized by a lower fluorescence quantum yield and lifetime if compared to **DTS**, exhibits a behavior similar to that of quaterthiophene: whereas k_F increases by a factor around 2 ($k_F=1.1 \times 10^8 \text{ s}^{-1}$ for **DTS** and $2.6 \times 10^8 \text{ s}^{-1}$ for **T1**), the sum of non-radiative constant increases by a factor around 100 ($k_{nr}=1.8 \times 10^7 \text{ s}^{-1}$ for **DTS** $2.8 \times 10^9 \text{ s}^{-1}$ for **T1**), giving to **T1** photophysical properties similar to those of the corresponding quaterthiophene ($k_F=4.1 \times 10^8 \text{ s}^{-1}$ and $k_{nr}=1.9 \times 10^9 \text{ s}^{-1}$ in benzene). **T2** resembles **T1** in the photophysical behavior. It was shown that the fluorescence quantum yields increase and the triplet quantum yields decrease as a function of the chain length in OTs.^[47] The calculated spin-orbit coupling strength together with the energy gaps between S_1 and the triplet state involved in intersystem crossing process account for such results: in particular, a fundamental role was attributed to the energy gap between S_1 and the T_2 or T_3 triplet states.^[54] It has been suggested that in bithiophene and higher OTs the non-planarity of the thiophene backbone increases the intersystem crossing efficiency. Therefore, the high fluorescence quantum yield shown by **DTS**, and hence the very low efficiency of the non-radiative paths, if compared to bithiophene, could be explained by the inhibition of the out-of-plane torsions in such a rigid structure. Furthermore, the longer and more flexible molecules (**T1**, **T2**, **E1** and **E2**) exhibit radiative and non-radiative constants similar to the correspondent OTs.

E1 and **E2** show further red-shifted absorption and emission spectra, due to the extended π -conjugation which involves also the DCV end caps (see the LUMOs of **E1** and **E2** in Figure S1). The role of electron-withdrawing DCV end groups in lowering the optical band gap of OTs has been studied: the absorption maximum of the terminally DCV-substituted sexithiophene without side chains is at 532 nm in dichloromethane^[55], not different from the value we found for **E1**. The effect of the substitution by the octyl chains on the absorption spectrum of **E1** in low polarity solvents (maximum at 532 nm) can be understood by a comparison with the correspondent compound lacking side alkyl chains (maximum at 542 nm).^[56] Such a finding could be explained by the twisting around interring single bonds induced by the steric hindrance of the alkyl substituents, which leads to conformations with a slightly reduced conjugation on the whole. On the other hand, the octylsulfanyl chain, if compared with the octyl one, induces a reduction of the band gap in **E2** (maximum at 557 in dichloromethane),

thanks also to the involvement of sulfur in π -conjugated system. These results confirm that the introduction of alkyl side chains acts by increasing the optical band gap; on the contrary, the **DTS** central core in **E1** and **E2** is still able to increase the π -conjugation length. In **E1** the positive effect of the **DTS** core is counterbalanced by the presence of the octyl chain, whereas in **E2** a reduction of the optical band gap, if compared to **E1** and also to the different DCV-substituted sexithiophenes reported in literature, [55, 56] can be observed, attributable to the stronger bathochromic effect induced by the alkylsulfanyl chain.

Table 2. Absorption and emission maxima, molar absorption coefficients, Stokes shifts, quantum yields (Φ_F) and fluorescence lifetimes (τ_F), radiative and overall non-radiative decay rate constants of **DTS**, **T1**, **T2**, **E1** and **E2**

Compound	Solvent	$\lambda_{\text{abs}}^{\text{max}}$ (nm)	$\lambda_{\text{fluo}}^{\text{max}}$ (nm)	Stokes shift (cm ⁻¹)	Φ_F	τ_F (ns)	k_F (s ⁻¹)	k_{nr} (s ⁻¹)
DTS	<i>n</i> -hexane	241,336	403	4950	0.86	7.75	1.1×10^8	1.8×10^7
		$(\epsilon^{\text{max}}=11100 \text{ M}^{-1}\text{cm}^{-1})$						
		FWMH=4530 cm ⁻¹	FWMH=3900 cm ⁻¹					
	dichloromethane	243,338	405	4890				
	acetonitrile	240,336	404	5010	0.89	8.42	1.1×10^8	1.3×10^7
T1	<i>n</i> -hexane	265,308,403	484,505	5010	0.087	0.33	2.6×10^8	2.8×10^9
		$(\epsilon^{\text{max}}=24900 \text{ M}^{-1}\text{cm}^{-1})$						
		FWMH=4770 cm ⁻¹	FWMH=3390 cm ⁻¹					
	dichloromethane	266,311,407	488,510	4960				
	acetonitrile	265,309,402	486,507	5150				
T2	<i>n</i> -hexane	270, ~325,434	495,520	3810	0.12	0.41	2.9×10^8	2.1×10^9
		$(\epsilon^{\text{max}}=34100 \text{ M}^{-1}\text{cm}^{-1})$						
		FWMH=4360 cm ⁻¹	FWMH=3250 cm ⁻¹					
	dichloromethane	~328, 438	503,528	3890				
	acetonitrile	268, ~328,433	500,524	4010				
E1	<i>n</i> -hexane	390, 512	620, 665 (shoulder)	3400	0.32	0.78	4.1×10^8	8.7×10^8
		$(\epsilon^{\text{max}}=55100 \text{ M}^{-1}\text{cm}^{-1})$						
		FWMH=5880 cm ⁻¹	FWMH=2390 cm ⁻¹					
	ethyl acetate	390, 513	705	5310	0.21	1.0	2.1×10^8	7.9×10^8
	tetrahydrofuran	390, 520	720	5340				
	dichloromethane	395, 533	765	5690	0.13	0.81	1.6×10^8	1.1×10^9
	acetone	390, 515	780	6600				
E2	<i>n</i> -hexane	365, 520	650	3850				
		$(\epsilon^{\text{max}}=55100 \text{ M}^{-1}\text{cm}^{-1})$						
		FWMH=6080 cm ⁻¹	FWMH=2560 cm ⁻¹					
	dichloromethane	375, 555	790	5300				

The relevant features of **E1** and **E2**, which differentiate them from the other compounds studied in the present work, can be understood by the comparison between the **E1** OMs and those of the corresponding compound lacking the DCV (Figure S1) and highlights the role of DCV groups in changing the electronic structures of **E1** and **E2**: indeed, in such molecules the HOMO-LUMO transition involves an intramolecular charge transfer from the DTS electron-donor unit to the DCV electron-acceptor groups.

The influence of the solvent polarity on absorption and emission spectra was studied in detail for **E1**. While **DTS**, **T1** and **T2** show optical and photophysical properties independent of the solvent, **E1** shows a weak absorption solvatochromism (Figure 2a) and fluorescence strongly affected by the solvent polarity (Figure 2b): a large positive solvatochromism characterizes the emission spectra, where a red shift of about 3300 cm^{-1} from a nonpolar solvent (*n*-hexane) to a polar solvent (acetone) is observed. The absorption and emission spectra could not be collected in more polar solvents like acetonitrile or DMSO due to the low solubility of the compound.

The examined compounds are non-centrosymmetric, so the electric dipole moments calculated (at B3LYP level for all the molecules) for the relaxed ground state are non-null by symmetry: the values obtained for **DTS**, **T1** and **T2** are 1.48 D, 0.34 D, 1.35 D, respectively. For **E1** a value of 10.94 D was obtained, whereas for the analog compound lacking the DCV substituents a value of 0.37 D was calculated. The dipole moment is normal to the long molecular axis, along the C_2 symmetry axis. The dramatic influence of the solvent polarity on the emission properties of **E1** (Figure 2b) can be interpreted in terms of a large change in the electric dipole moment upon photoexcitation; however, the calculated value of the dipole moment of the Franck-Condon S_1 state is 12.93 D, indicating an increase of only 1.99 D. This computational finding is in agreement with the weak absorption solvatochromism but it does not permit to rationalize the relevant fluorescence solvatochromism observed. For the purpose of elucidating such behavior, the emission solvatochromism was experimentally studied for **E1** in five solvents of increasing polarity, from *n*-hexane to acetone. Using the Lippert-Mataga equation, a linear fit with a slope of 10770 cm^{-1} was obtained (Figure S2), considering a cavity radius $a=15\text{ \AA}$, so that the **E1** molecule is fully embedded in the model spherical cavity. This slope value corresponds to an increase of the dipole moment upon excitation of about 60 D. Though this value is probably overestimated, due to the non-spherical shape of the investigated molecule, the marked positive emission solvatochromic effect, along with the small difference of the dipole moment calculated between S_0 and the unrelaxed S_1 state, suggests an important increase of the S_1 polarity after relaxation.

Such a behavior, a weak positive absorption solvatochromism and a marked positive emission solvatochromism, is characteristic of several quadrupolar molecules and it has been widely reported in

literature.^[15, 57] Though these chromophores, because of their symmetric structure, are characterized by a low dipole moment in the ground state (a null dipole in the case of centrosymmetric molecules), which is maintained after the vertical transition, the strong emission solvatochromism suggests, on the contrary, the occurrence of a polar S_1 state. It has been interpreted on the basis of the excited-state symmetry breaking model induced by the solvent polarity: the first electronic excited state is characterized by the charge localization on one arm of the molecule, so that the emission originates from a polar state stabilized in polar solvents. We propose that this model, already used in order to explain the positive emission solvatochromism in V-shaped molecules,^[58] can effectively apply to these pseudo-quadrupolar dithienosilole-based molecules.

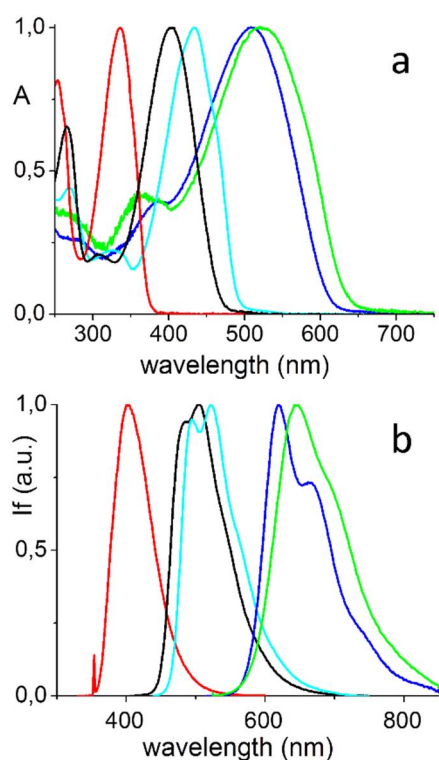


Figure 1. a) Normalized absorption spectra and b) corrected normalized fluorescence spectra of **DTS** (red), **T1** (black), **T2** (cyan), **E1** (blue), **E2** (green) in *n*-hexane

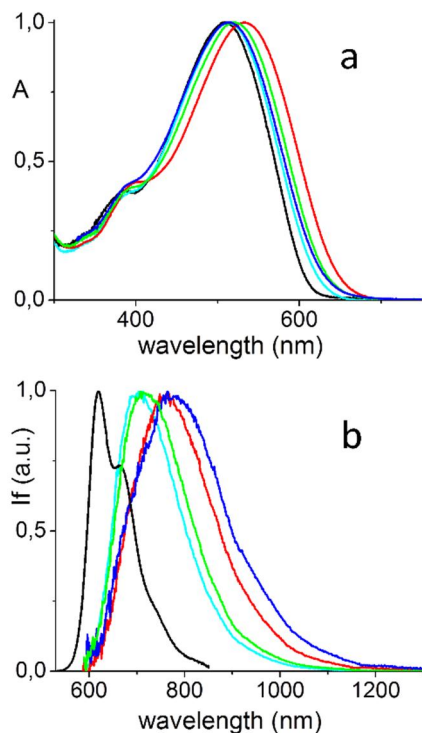


Figure 2. a) Normalized absorption spectra and b) corrected normalized fluorescence spectra of **E1** in *n*-hexane (black), ethyl acetate (cyan), tetrahydrofuran (green), dichloromethane (red), acetone (blue)

Electrochemical characterization

CV is a convenient research tool for the study of the electrochemical properties of molecules and other compounds, among which conducting oligomers and polymers, which can undergo oxidation and reduction processes.

The electrochemical parameters of **DTS**, **T1**, **T2**, **E1** and **E2** are reported in Table 3. All the compounds investigated in this study undergo a p-doping process exhibiting, with the exception of **DTS**, two reversible oxidation waves (I and II) attributable to the formation of cationic and dicationic sites. Figure 3 reports the voltammetric curves of oligomers **E1** and **E2**, while those of **DTS**, **T1** and **T2** can be found in Figure S3.

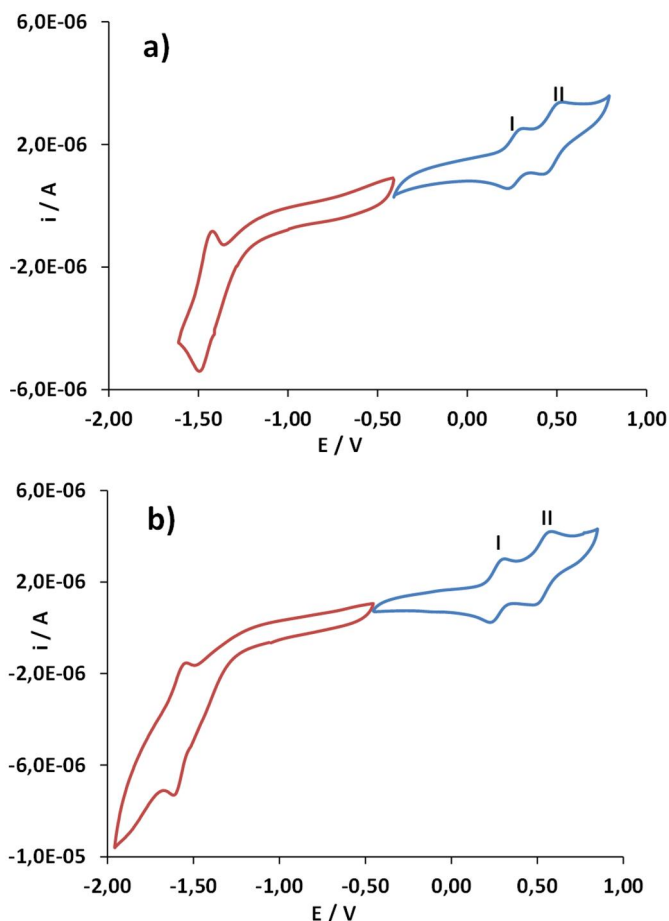


Figure 3. CV scan of a) **E1** and b) **E2** in a 0.1 M solution of TBAPF₆ in dichloromethane, at 100 mV/s scan rate.

The potential peak values relative to the first oxidation process ($E^{P_{oxI}}$) of **E1** and **E2**, as well as those of **T1** and **T2**, are very closed to each other, as reported in Table 3. Comparing the data relative to the second oxidation process ($E^{P_{oxII}}$), a more marked difference is notable especially between **T1** and **T2**. In the experimental conditions used for this study, it was possible to observe the occurrence of n-doping only with **E1** and **E2**; Figure 3 shows the relevant voltammetric curves. In this case, the peak potential of **E1** is located at less cathodic values with respect to **E2** (see Table 3).

From the CV curves recorded during oxidation and reduction processes is possible to determine the onset potentials, indicated as $E^{onset_{ox}}$ and $E^{onset_{red}}$, respectively. On the basis of these values, the electrochemical band gap ($E_{g_{electr}}$) energies can be derived (Table 3).

The obtained $E_{g_{electr}}$ values for **E1** and **E2** are consistent with those reported in the first column of Table 1. In particular, and in accordance to photochemical evidences and to theoretical calculations, $E_{g_{electr}}$ of **E2** is slightly narrower than that of **E1**.

Table 3: Electrochemical parameters of the studied oligomers in dichloromethane

	$E_{\text{onset}_{\text{ox}}}^{\text{ox}} \text{ (V)}$	$E_{\text{oxi}}^{\text{oxi}} \text{ (V)}$	$E_{\text{oxil}}^{\text{oxil}} \text{ (V)}$	$E_{\text{onset}_{\text{red}}}^{\text{red}} \text{ (V)}$	$E_{\text{red}}^{\text{red}} \text{ (V)}$	$E_{\text{electr}}^{\text{electr}} \text{ (eV)}$
DTS	+0.58	+0.72	+0.84	/	/	/
T1	+0.22	+0.34	+0.72	/	/	/
T2	+0.22	+0.32	+0.62	/	/	/
E1	+0.20	+0.31	+0.59	-1.53	-1.63	1.73
E2	+0.22	+0.33	+0.55	-1.41	-1.48	1.63

Conclusions

Two A- -D- -A thiophene-based small molecules, having a central electron-donating dithienosilole unit and terminal electron-withdrawing methyl-DCV units, differing only for the substitution at the thiophene ring (**E1** bearing a *n*-octyl chain vs **E2** bearing a *n*-octylsulfanyl chain), were synthesized. The spectroscopic, photophysical and electrochemical properties of **E1**, **E2** and of their precursors (**DTS**, **T1** and **T2**) were studied. In particular, the influence of the nature of the building blocks and substituents on the optical and photophysical properties was rationalized in order to gain further insights into the design of materials for applications in optoelectronic devices. A first conclusion is that the central rigid dithienosilole unit allows for an increased π -conjugation length and hence a lower optical band-gap if compared to the correspondent oligothiophenes lacking the dithienosilole central unit.

A progressive bathochromic shift in absorption and emission spectra is observed by passing from **DTS** to **T1** and **T2**; **E1** and **E2** exhibit a further red-shifted absorption. The TDDFT calculations show that the lowest-energy absorption band is mainly attributable to the HOMO-LUMO transition for all compounds; they are characterized by an extended π -conjugation, involving in **E1** and **E2** also the terminal DCV groups. **DTS** exhibits a peculiar photophysical behavior, if compared with that of 2,2'qbitiophene: it is characterized by a very high fluorescence quantum yield and not efficient non-radiative deactivation paths. On the contrary, longer and more flexible molecules **T1**, **T2**, **E1** and **E2** show a photophysical behavior similar to that of the correspondent OTs, with similar radiative and non-radiative constants. The relevant features of **E1** and **E2**, which exhibit different optical and photophysical properties if compared with their precursors, were highlighted: in such molecules the HOMO-LUMO transition involves a intramolecular charge transfer from the electron-donor dithienosilole unit to the two terminal electron-acceptor DCV groups. The optical and photophysical properties are independent of the solvent for **DTS**, **T1** and **T2**, whereas a marked positive emission

solvatochromism is shown by **E1** and **E2**: the increased electric dipole moment upon photoexcitation in such two quadrupolar-like molecules can be interpreted on the basis of the symmetry breaking in the S_1 excited state.

The role of the octylsulfanyl lateral chains in reducing the optical band. gap in **T2** and **E2** with respect to that shown in compounds bearing octyl chains (**T1** and **E1**) is due both to electronic and conformational effects related to the presence of the sulfur atom. Electrochemical data confirm the decrease of the electronic band-gap going from **E1** to **E2**. Finally, the significant deshielding of the ^1H NMR proton signal of the central dithienosilole unit in **T2** with respect to **DTS** and **T1**, is in favor of a more planar conformation of **T2** with respect to **T1** in solution.

Experimental section

Synthesis: 3-octylthiophene was purchased from Sigma Aldrich, 2-bromo-3-octylthiophene was obtained as already reported.^[59] 2-bromo-3-octylsulfanylthiophene was obtained as reported in ref.^[60] Medium Pressure Liquid Chromatography (MPLC) was performed with a Grace Reveleris Flash Chromatography system with evaporative light scattering (Alltech 3300 ELSD) and UV detection. ^1H and ^{13}C NMR spectra were recorded with Bruker Avance 400 and Avance III HD 600 spectrometers, operating at 400.13 and 600.13 for proton and at 100.61 and 150.90 MHz for carbon, respectively, Assignments were made applying standard HSQC and HMBC pulse sequences.

Computational Details: All the calculations on molecules **DTS**, **T1**, **T2**, **E**, **E1** and **E2** were carried out (without the inclusion of solvent effects) using both Firefly Quantum Chemistry package,^[61] which is partially based on the GAMESS (US) source code^[62], as well as NWChem package^[63]. Assuming for all the molecules a model C_2 starting structure, the ground state geometry was fully optimized at DFT B3LYP/Ahalrichs-pVDZ level. We also checked for the positive semidefinite character of the nuclear hessian in order to ensure that the located stationary point was a true local minimum. Starting from these gas-phase optimized structures, the Kohn-Sham (KS) HOMO and LUMO orbital energies were employed for evaluating the KS gap ($\epsilon_{\text{HOMO}}^{\text{KS}} - \epsilon_{\text{LUMO}}^{\text{KS}}$) which is an approximation of the fundamental electronic gap E_g . The basis set Ahalrichs-pVDZ was also used for the calculation of the optical one-photon absorption (OPA) spectra in the framework of adiabatic LR-TDDFT exploiting both B3LYP as well as CAM-B3LYP functionals.

Optical and photophysical properties: UV-vis spectra were collected using a Varian Cary 100 Scan UV-vis spectrophotometer. Fluorescence measurements were performed on a Horiba Jobin Yvon Fluoromax-3

spectrofluorometer. Emission spectra extending into the NIR region were obtained with an Edinburgh Instruments FLS920 spectrometer equipped with a Hamamatsu R5509-72 supercooled photomultiplier tube. Spectra were corrected for the instrumental spectral sensitivity. Fluorescence quantum yields (Φ) were determined at $T = 20.25$ °C using different standards: 9,10-diphenyl-anthracene in cyclohexane ($\Phi = 0.90$ [64] for **DTS**, quinine sulfate in H_2SO_4 1N ($\Phi = 0.545$ [64]) for **T1**, fluoresceine in NaOH 0.1 M for **T2** ($\Phi = 0.925$ [65]) and cresyl violet in methanol ($\Phi = 0.64$ [66]) for **E1**. The correction for the refractive index of the solvents was introduced. Fluorescence lifetimes were measured with a Horiba FluoroMax4 time correlated single-photon counting equipment using as excitation sources different nano-LEDs, emitting at 340 nm for **DTS**, 450 nm for **T1** and **T2**, 570 nm for **E1** and **E2**. Emission experiment were performed on solutions deoxygenated by bubbling nitrogen.

Electrochemical measurements: the electrochemical properties were investigated by cyclic voltammetry (CV) in a dichloromethane solution containing tetraethylammonium hexafluorophosphate ($TEAPF_6$) (puriss., Fluka) as the supporting electrolyte. The measurements were carried out in a three electrodes cell in a dry argon atmosphere using an Autolab PGSTAT 12 galvanostat/potentiostat (Eco Chemie). A 3-mm-diameter Pt disk (Metrohm) was used as the working electrode. A platinum wire and a silver wire covered with AgCl were the auxiliary and the pseudo-reference electrodes, respectively. The potential of the pseudo-reference electrode with respect to the ferrocene/ferrocenium (Fc/Fc^+) redox couple was always measured after each experiment.

Synthesis of 3,3-dibromo-5,5-bis(trimethylsilyl)-2,2-bithiophene: this compound was obtained as already reported [37]

Synthesis of **DTS:** in a round bottom Schlenk tube a solution of 3,3-dibromo-5,5-bis(trimethylsilyl)-2,2-bithiophene (1.5 g, 3.20 mmol) in 15 mL of dry THF was cooled to -78 °C under nitrogen atmosphere. *n*-Butyllithium (1.6 M in hexane, 4.6 mL, 7.36 mmol) was added dropwise to the cooled solution and stirring was prolonged for 1 h at -78 °C. Then, 1.33 mL (3.84 mmol) of dichlorodioctylsilane were added dropwise to the solution and stirring prolonged for 3 h at room temperature. The mixture was diluted with diethyl ether (15 mL), washed with a saturated solution of NaCl (2×15 mL) and water (2×15 mL), and dried over $MgSO_4$. After removal of the solvent under reduced pressure, the NMR spectra of the brown oil thus obtained revealed the presence of **DTS** as the major compound with some impurities attributable to its fully and partially deprotected analogues. The crude was therefore dissolved in 80 mL of chloroform and treated with trifluoroacetic acid (0.6 mL, slow addition) for 3 h at room temperature. The mixture was then washed with water (50 mL), dried over $MgSO_4$ and the solvent removed under reduced pressure giving a brown oil. The crude was purified via MPLC

using a prepacked column of 24 g of silica and *n*-hexane as the eluent, obtaining a yellow oil (0.83 g, 53% yield). ¹H NMR (600 MHz, CDCl₃): = 7.20 (d, J = 4.7 Hz, 1H), 7.05 (d, J = 4.7 Hz, 1H), 1.38 (m, 2H), 1.32-1.17 (m, 10H), 0.89 (m, 2H), 0.87 ppm (t, J = 7.0 Hz, 3H); ¹³C NMR (600 MHz, CDCl₃): = 149.2, 141.6, 129.6, 124.9, 33.1, 31.8, 29.2, 29.1, 24.2, 22.6, 14.1, 11.9 ppm.

Synthesis of 1: in a round bottom flask protected from light, *N*-bromosuccinimide (0.37 g, 2.09 mmol) was added portionwise to a solution of **1** (0.4 g, 0.95 mmol) in 25 mL of chloroform. The solution was stirred for 5 h at room temperature then washed with water (2×25 mL), dried over MgSO₄, filtered and the solvent removed under reduced pressure. The crude was purified by MPLC on silica gel, using petroleum ether 40-60 as eluent, affording 0.387 g of a green viscous oil (70% yield) of **1**. ¹H NMR (400 MHz, CDCl₃): = 6.99 (s, 1H), 1.39-1.17 (m, 12H), 0.86 (m, 2H), 0.88 ppm (t, J = 7.1 Hz, 3H); ¹³C NMR (400 MHz, CDCl₃): = 148.8, 140.9, 132.2, 111.1, 33.1, 31.8, 29.2, 29.1, 24.0, 22.6, 14.1, 11.6 ppm.

Synthesis of 2a: in a round bottom Schlenk tube and under argon atmosphere, a solution of 2-bromo-3-octylthiophene (2.7 g, 9.8 mmol) in 50 mL of anhydrous THF was cooled to -78 °C. A solution of *n*-butyllithium (6.44 mL, 1.6 M in hexane) was dropwise added and the mixture stirred for 2 h, then 2-isopropoxy-4,4,5,5-tetramethyl-1,3,2-dioxaborolane (4 mL, 19.6 mmol) was slowly added. The chiller was switched off and the mixture stirred overnight. The solution was washed with 50 mL of a saturated solution of NaHCO₃, extracted with ethyl acetate (2×30 mL), washed with water (2×50 mL), dried over MgSO₄ and concentrated under reduced pressure. The crude was purified by MPLC on silica gel column (neutralized with trimethylamine, and gradient elution from 100% *n*-hexane to *n*-hexane ethyl acetate 90:10) to yield an oil (1.7 g, 54%). ¹H NMR (400 MHz, CDCl₃): = 7.48 (d, J = 4.7 Hz, 1H), 7.01 (d, J = 4.7 Hz, 1H), 2.88 (t, J = 7.6, 2H), 1.56 (m, 2H), 1.33 (s, 12H), 1.32-1.21 (m, 10H), 0.88 (t, J = 6.7 Hz).

Synthesis of 2b: was prepared in the same way as **2a**, starting from 2-bromo-3-octylsulfanyliothiophene (1.05 g, 3.81 mmol) obtaining a crude (24% yield) which decomposes on neutralized silica and alumina and therefore was used as obtained for the next step. ¹H NMR (400 MHz, CDCl₃): = 7.55 (d, J = 4.9 Hz, 1H), 7.09 (d, J = 4.9 Hz, 1H), 2.94 (t, J = 7.5 Hz, 2H), 1.63 (qn, J=7.5 Hz, 2H), 1.41 (m, 2H), 1.35 (s, 12H), 1.33-1.21 (m, 8H), 0.89 (t, J = 6.9 Hz, 3H); ¹³C NMR (400 MHz, CDCl₃): = 143.5, 131.7, 129.7, 126.3, 34.9, 31.9, 29.5, 29.2, 28.9, 24.8, 22.6, 14.1 ppm.

Synthesis of T1: in a round bottom Schlenk tube, a solution of **1** (0.37 g, 0.64 mmol) and **2a** (0.522 g, 1.62 mmol) in toluene (10 mL) and ethanol (1 mL) was degassed. In another Schlenk tube a solution of Na₂CO₃ (2 M in water, 2.4 mL) was degassed with repeated vacuum/argon cycles for 30 min. To the first Schlenk tube the catalyst tetrakis(triphenylphosphine)palladium(0) (0.073 g, 0.064 mmol) was added and the solution of

carbonate was slowly cannulated. The mixture was refluxed overnight, cooled to room temperature, poured in water (10 mL), extracted with *n*-hexane (2×10mL) and washed with water. The organic phases were dried over MgSO₄, filtered and concentrated. The sticky solid obtained was washed with methanol and purified by MPLC on silica gel and petroleum ether:ethyl acetate 90:10 as the eluent, obtaining 0.42 g (81%) of a dark yellow viscous liquid. ¹H NMR (600 MHz, CDCl₃): = 7.16 (d, J = 5.1 Hz, 1H), 7.05 (s, 1H), 6.93 (d, J = 5.1 Hz, 1H), 2.78 (t, J = 7.8, 2H), 1.65 (qn, J=7.6, 2H), 1.42 (m, 2H), 1.37 (m, 2H), 1.35-1.18 (m, 18H), 0.94 (m, 2H), 0.87 (t, J = 7.0 Hz, 3H), 0.86 (t, J = 7.1 Hz, 3H); ¹³C NMR (400 MHz, CDCl₃): = 148.8, 142.0, 139.3, 136.7, 131.0, 130.0, 128.6, 123.4, 33.2, 31.9, 30.6, 29.5, 29.4, 29.3, 29.2, 24.2, 22.7, 14.1, 11.8 ppm.

Synthesis of T2: The title compound was prepared in the same way as **T1** obtaining 180 mg (71% yield) of an orange viscous liquid starting from 0.17 g of **1**. ¹H NMR (600 MHz, CDCl₃): = 7.32 (s, 1H), 7.14 (d, J = 5.3 Hz, 1H), 7.03 (d, J = 5.3 Hz, 1H), 2.85 (t, J = 7.4, 2H), 1.61 (qn, J=7.5, 2H), 1.40 (m, 4H), 1.36-1.18 (m, 18H), 0.94 (m, 2H), 0.85 (2 t, J = 6.8 Hz, 6H); ¹³C NMR (600 MHz, CDCl₃): = 149.9, 141.7, 136.8, 136.2, 132.5, 128.9, 127.0, 122.4, 36.1, 33.2, 31.7, 29.6, 29.1, 28.7, 24.1, 22.6, 14.0, 11.7 ppm.

Synthesis of 3a: in a round bottom Schlenk tube a solution of **T1** (0.12 g, 0.15 mmol) in THF (5 mL) was cooled to -78°C and three cycles, consisting of lithium diisopropylamide (1 M in THF/*n*-hexane, 0.18 mL, 0.18 mmol) dropwise addition, followed by a 40 min stirring period and by a dropwise addition of a solution of trimethyltin chloride in *n*-hexane (1 M, 0.18 mL, 0.18 mmol), were repeated. After the last addition of trimethyltin chloride, stirring was prolonged for 30 min at -78 °C. The solution was left under stirring for 1 h and a half at 30 °C then for 30 min at room temperature. Water (5 mL) was added then the mixture was extracted with *n*-hexane (2×5 mL) and the organic phases washed with water (2×5 mL) and dried over Na₂SO₄. After removal of the solvent, a yellow-green viscous oil (0.14 mg, 82% yield) was obtained and used as it was for the next step. ¹H NMR (600 MHz, acetone-d₆): = 7.22 (s, 1H), 7.12 (s, 1H), 2.83 (t, J = 7.6, 2H), 1.68 (qn, J=7.6, 2H), 1.48 (m, 2H), 1.41 (m, 2H), 1.37-1.20 (m, 18H), 1.04 (m, 2H), 0.87 (t, J = 7.0 Hz, 3H), 0.85 (t, J = 7.1 Hz, 3H), 0.38 (s, 9H, J_{H,Sn} = 56.6, 58.8 Hz); ¹³C NMR (600 MHz, CDCl₃): = 149.0, 143.5, 141.4, 139.6, 138.1, 137.6, 137.0, 129.2, 33.6, 32.6, 32.7, 31.4, 30.0, 29.9, 29.8, 29.6, 24.9, 23.4, 14.4, 12.3, -8.3 ppm.

Synthesis of 3b: The title compound was prepared in the same way as **3a** obtaining 160 mg (90% yield) of an orange viscous liquid starting from 0.91 g of **T2**. ¹H NMR (400 MHz, acetone-d₆): = 7.52 (s, 1H), 7.26 (s, 1H), 2.98 (t, J = 7.1, 2H), 1.65 (qn, J=7.6, 2H), 1.48 (m, 2H), 1.41-1.22 (m, 20H), 1.04 (m, 2H), 0.88 (m, 6H), 0.45 (s, 9H, J_{H,Sn} = 56.9, 58.3 Hz).

Synthesis of 4: in a round bottom flask hexamethyldisilazane (1.42 g, 8.7 mmol) was slowly added to 4.8 mL of acetic acid, keeping the temperature below 75° C. The hexamethyldisilazane/acetic acid mixture was then

added dropwise to a flask containing a solution of 2-acetyl-5-bromothiophene (1.5 g, 7.31 mmol) and malononitrile (0.97 g, 14.63 mmol) in 2.4 mL of acetic acid. The mixture was stirred at 65 °C for 22 h, then cooled to room temperature with chilled toluene (12 mL) and diluted with water (9 mL). The aqueous layer was separated and extracted with toluene (5 mL). The combined organic extracts were washed with water (4x5mL) and dried over MgSO₄. After removal of the solvent and recrystallization from methanol a yellow solid was obtained (0.68 g, 37% yield). ¹H NMR (600 MHz, CDCl₃): = 7.76 (d, J = 4.3 Hz, 1H), 7.22 (d, J = 4.3 Hz, 1H), 2.64 (s, 3H); ¹³C NMR (600 MHz, CDCl₃): = 161.0, 139.3, 134.1, 132.0, 123.7, 113.8, 113.3, 79.0, 23.0.

Synthesis of E1: in a round bottom Schlenk tube a solution of **3a** (0.11 g, 0.097 mmol) and **4** (0.054 g, 0.213 mmol) in dry toluene (5.5 mL) was degassed with argon and vacuum followed by the addition of Pd(PPh₃)₄ (4 mg, 0.034 mmol). After stirring at 110 °C for 24 h under inert atmosphere, the mixture was poured into water (30 mL), and extracted with chloroform. The organic layer was washed with water (2x20 mL), dried over Na₂SO₄, reduced at small volume and reprecipitated with methanol. The solid obtained was filtered in a cellulose thimble in a Soxhlet apparatus, washed with methanol and extracted with chloroform. After removal of the solvent, 105 mg (76% yield) of a black solid were obtained. Elemental analysis calcd (%) for C₆₆H₈₂N₄S₆ (1150.5): C 68.82, H 7.18, N 4.86, S 16.70; found: C 68.69, H 7.20, N 4.88, S 16.64. ¹H NMR (600 MHz, CDCl₃): = 7.95 (d, J = 4.2 Hz, 1H), 7.24 (d, J = 4.2 Hz, 1H), 7.23 (s, 1H), 7.16 (s, 1H), 2.80 (t, J = 7.8, 2H), 2.68 (s, 3H), 1.70 (qn, J=7.6, 2H), 1.42 (m, 4H), 1.39-1.20 (m, 18H), 0.97 (m, 2H), 0.88 (t, J = 7.0 Hz, 3H), 0.86 (t, J = 7.0 Hz, 3H); ¹³C NMR (400 MHz, CDCl₃): = 160.9, 149.4, 146.8, 143.1, 140.7, 136.1, 135.7, 135.4, 134.0, 132.2, 129.7, 129.2, 124.6, 114.6, 114.0, 76.8, 33.1, 31.9, 30.4, 29.6, 29.5, 29.4, 29.2, 24.2, 23.0, 22.7, 14.1, 11.7 ppm.

Synthesis of E2 The title compound was prepared in the same way as **E1** obtaining 0.08 g (48% yield) of a black solid starting from 0.16 g of **3b**. Elemental analysis calcd (%) for C₆₆H₈₂N₄S₈ (1215.9): C 65.19, H 6.80, N 4.61, S 21.10; found: C 65.03, H 6.83, N 4.59, S 21.02. ¹H NMR (600 MHz, CDCl₃): = 7.96 (d, J = 4.3 Hz, 1H), 7.40 (s, 1H), 7.30 (s, 1H), 7.25 (d, J = 4.3 Hz, 1H), 2.92 (t, J = 7.4, 2H), 2.68 (s, 3H), 1.67 (qn, J=7.4, 2H), 1.43 (m, 4H), 1.38-1.20 (m, 18H), 0.96 (m, 2H), 0.85 (t, J = 6.8 Hz, 6H); ¹³C NMR (400 MHz, CDCl₃): = 160.9, 150.9, 145.8, 142.8, 138.8, 136.1, 136.0, 135.2, 131.5, 131.3, 129.7, 128.9, 124.8, 114.4, 113.6, 77.2, 36.5, 33.2, 31.9, 31.8, 29.6, 29.3, 29.1, 28.8, 24.2, 23.1, 22.7, 22.6, 14.1, 11.8 ppm.

Acknowledgements

The authors wish to thank Dr. Filippo Monti (Institute of Organic Synthesis and Photoreactivity - CNR Bologna) for his assistance in collecting the fluorescence spectra in the NIR range.

Keywords: electrochemistry ~ fluorescence ~ oligothiophenes ~ photophysics ~ solvatochromism

Reference

- [1] I. F. Perepichka, D. F. Perepichka, *Handbook of Thiophene-Based Materials : Applications in Organic Electronics and Photonics*, Wiley, **2009**.
- [2] W. Wu, A. Chen, L. Tong, Z. Qing, K. P. Langone, W. E. Bernier, W. E. Jones, *ACS Sensors* **2017**, *2*, 1337. 1344.
- [3] B. Huang, Z. Geng, S. Yan, Z. Li, J. Cai, Z. Wang, *Anal. Chem.* **2017**, *89*, 8816. 8821.
- [4] M. J. Kim, A.-R. Jung, M. Lee, D. Kim, S. Ro, S.-M. Jin, H. D. Nguyen, J. Yang, K.-K. Lee, E. Lee, M. S. Kang, H. Kim, J.-H. Choi, B. S. Kim, J. H. Cho, *ACS Appl. Mater. Interfaces* **2017**, *9*, 40503. 40515.
- [5] M. Amaresh, B. Peter, *Angew. Chemie Int. Ed.* **2012**, *51*, 2020. 2067.
- [6] L. Zhang, N. S. Colella, B. P. Cherniawski, S. C. B. Mannsfeld, A. L. Briseno, *ACS Appl. Mater. Interfaces* **2014**, *6*, 5327. 5343.
- [7] Z. Wang, L. Zhu, Z. Shuai, Z. Wei, *Macromol. Rapid Commun.* **2017**, *38*, 1700470.
- [8] M. Mazzeo, F. Mariano, G. Gigli, G. Barbarella, *Organic Light Emitting Diodes Based on Functionalized Oligothiophenes for Display and Lighting Applications*, ISBN: 978-953-307-140-4, IntechOpen **2010**. Available from: <http://www.intechopen.com/books/organic-light-emitting-diode>
- [9] A. R. Murphy, J. M. J. Fréchet, *Chem. Rev.* **2007**, *107*, 1066. 1096.
- [10] L. Yan, C. Li, L. Cai, K. Shi, W. Tang, W. Qu, C.-L. Ho, G. Yu, J. Li, X. Wang, *J. Organomet. Chem.* **2017**, *846*, 269. 276.
- [11] J. Shi, L. Xu, Y. Li, M. Jia, Y. Kan, H. Wang, *Org. Electron.* **2013**, *14*, 934. 941.
- [12] J. Roncali, *Chem. Rev.* **1997**, *97*, 173-205.
- [13] J. M. Hales, S. H. Chi, V. W. Chen, J. W. Perry, *Materials and Energy* **2016**, *7*(WSPC Reference on Organic Electronics: Organic Semiconductors, Volume 2: Fundamental Aspects of Materials and Applications), 397-442.

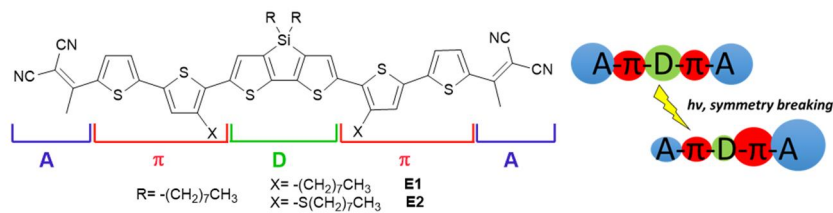
- [14] F. Ricci, B. Carlotti, B. Keller, C. Bonaccorso, C. G. Fortuna, T. Goodson III, F. Elisei, A. Spalletti, J. *Phys. Chem. C* **2017**, *121*, 3987–4001.
- [15] F. Terenziani, A. Painelli, C. Katan, M. Charlot, M. Blanchard-Desce, *J. Am. Chem. Soc.* **2006**, *128*, 15742-15755.
- [16] A. Mishra, C. Urich, E. Reinold, M. Pfeiffer, P. Bäuerle, *Adv. Energy Mater.* **2011**, *1*, 265–273.
- [17] M. Weidelener, C. D. Wessendorf, J. Hanisch, E. Ahlswede, G. Götz, M. Lindén, G. Schulz, E. Mena-Osteritz, A. Mishra, P. Bäuerle, *Chem. Commun.* **2013**, *49*, 10865.
- [18] G. L. Schulz, M. Löbert, I. Ata, M. Urdanpilleta, M. Lindén, A. Mishra, P. Bäuerle, *J. Mater. Chem. A* **2015**, *3*, 13738–13748.
- [19] I. Ata, S. Ben Dkhil, M. Pfannmöller, S. Bals, D. Duché, J.-J. Simon, T. Koganezawa, N. Yoshimoto, C. Vidélot-Ackermann, O. Margeat, O. Margeat, J. Ackermann, P. Bäuerle, *Org. Chem. Front.* **2017**, *4*, 1561–1573.
- [20] B. Walker, S. Yum, B. Jang, J. Kim, T. Kim, J. Y. Kim, H. Y. Woo, *RSC Adv.* **2016**, *6*, 77655–77665.
- [21] J. Ohshita, *Macromol. Chem. Phys.* **2009**, *210*, 1360–1370.
- [22] D. Ye, X. Li, L. Yan, W. Zhang, Z. Hu, Y. Liang, J. Fang, W.-Y. Wong, X. Wang, *J. Mater. Chem. A* **2013**, *1*, 7622-7629.
- [23] J. Wu, Y. Ma, N. Wu, Y. Lin, J. Lin, L. Wang, C.-Q. Ma, *Org. Electron.* **2015**, *23*, 28–38.
- [24] S. Paek, J. K. Lee, J. Ko, *Sol. Energy Mater. Sol. Cells* **2014**, *120*, 209–217.
- [25] J. Min, Y. N. Luponosov, C. Cui, B. Kan, H. Chen, X. Wan, Y. Chen, S. A. Ponomarenko, Y. Li, C. J. Brabec, *Adv. Energy Mater.* **2017**, *7*, 1700465.
- [26] Y. N. Luponosov, J. Min, T. Ameri, C. J. Brabec, S. A. Ponomarenko, *Org. Electron.* **2014**, *15*, 3800–3804.
- [27] P. Morvillo, F. Parenti, R. Diana, C. Fontanesi, A. Mucci, F. Tassinari, L. Schenetti, *Solar Energy Materials & Solar Cells* **2012**, *104*, 45–52.

- [28] F. Parenti, R. Ricciardi, R. Diana, P. Morvillo, C. Fontanesi, F. Tassinari, L. Schenetti, C. Minarini, A. Mucci. *J. Polym. Sci.* **2016**, *54*, 1603. 1614.
- [29] F. Parenti, P. Morvillo, E. Bobeico, R. Diana, M. Lanzi, C. Fontanesi, F. Tassinari, L. Schenetti, A. Mucci, *Eur. J. Org. Chem.* **2011**, 5659. 5667.
- [30] R. Cagnoli M. Caselli, E. Libertini, A. Mucci, F. Parenti, G. Ponterini, L. Schenetti, *Polymer* **2012**, *53*, 403. 410.
- [31] C. Cui, W.-Y. Wong, Y. Li, *Energy Environ. Sci.* **2014**, *7*, 2276-2284.
- [32] Lisa M. Kozycz, Dong Gao, Jon Hollinger, Dwight S. Seferos, *Macromolecules* **2012**, *45*, 5823 5832.
- [33] R. Grisorio, G. P. Suranna, P. Mastrorilli, G. Allegretta, A. Loiudice, A. Rizzo, G. Gigli, K. Manoli, M. Magliulo, L. Torsi, *J. Polym. Sci. Part A Polym. Chem.* **2013**, *51*, 4860. 4872.
- [34] P. M. Beaujuge, H. N. Tsao, M. R. Hansen, C. M. Amb, C. Risko, J. Subbiah, K. R. Choudhury, A. Mavrinskiy, W. Pisula, J.-L. Brédas, F. So, K. Müllen, J. R. Reynolds, *J. Am. Chem. Soc.* **2012**, *134*, 8944. 8957.
- [35] S. Subramaniyan, H. Xin, F. S. Kim, S. A. Jenekhe, *Macromolecules* **2011**, *44*, 6245. 6248.
- [36] L. Sz-Yu, K. Chi-Shiang, C. Jhieh-Han, L. Yun-Wen, K. Shih-Yu, C. You-Hong, F. Chia-Chia, W. Chang-Yi, C. Chao-Ming, C. Yang-Hsiang, *ACS Macro Lett.* **2016**, *5*, 154-157.
- [37] Y. A. Getmanenko, P. Tongwa, T. V. Timofeeva, S. R. Marder, *Org. Lett.* **2010**, *12*, 2136. 2139.
- [38] L. Liao, L. Dai, A. Smith, M. Durstock, J. Lu, J. Ding, Y. Tao, *Macromolecules* **2007**, *40*, 9406. 9412.
- [39] J. Hou, H.-Y. Chen, S. Zhang, G. Li, Y. Yang, *J. Am. Chem. Soc.* **2008**, *130*, 16144. 16145.
- [40] P. M. Beaujuge, W. Pisula, H. N. Tsao, S. Ellinger, K. Müllen, J. R. Reynolds, *J. Am. Chem. Soc.* **2009**, *131*, 7514. 7515.
- [41] M. M. M. Raposo, A. M. C. Fonseca, G. Kirsch, *Tetrahedron* **2004**, *60*, 4071. 4078.
- [42] H. Ziehlke, R. Fitzner, C. Koerner, R. Gresser, E. Reinold, P. Bäuerle, K. Leo, M. K. Riede, *J. Phys. Chem. A* **2011**, *115*, 8437. 8446.

- [43] M. S. Wrackmeyer, M. Hummert, H. Hartmann, M. K. Riede, K. Leo, *Tetrahedron* **2010**, *66*, 8729-8733.
- [44] D. M. Barnes, A. R. Haight, T. Hameury, M. A. McLaughlin, J. Mei, J. S. Tedrow, J. D. Riva Toma, *Tetrahedron* **2006**, *62*, 11311-11319.
- [45] X. Zhan, S. Barlow, S. R. Marder, *Chem. Commun.* **2009**, 1948-1955.
- [46] Z. Fei, Y. Kim, J. Smith, E. Buchaca Domingo, N. Stingelin, M. A. McLachlan, K. Song, T. D. Anthopoulos, M. Heeney, *Macromolecules* **2012**, *45*, 735-742.
- [47] R.S. Becker, J. Seixas de Melo, A. L. Maçanita, F. Elisei, *J. Phys. Chem.* **1996**, *100*, 18683-18695.
- [48] G. Macchi, B. Milián Medina, M. Zambianchi, R. Tubino, J. Cornil, G. Barbarella, J. Gierschner, F. Meinardi, *Phys. Chem. Chem. Phys.* **2009**, *11*, 984-990.
- [49] P.F. van Hutten, R. E. Gill, J. K. Herrema, G. Hadziioanno, *J. Phys. Chem.* **1995**, *99*, 3218-3224.
- [50] D. Iarossi, A. Mucci, L. Schenetti, R. Seeber, F. Goldoni, M. Affronte, F. Nava, *Macromolecules* **1999**, *32*, 1390-1397.
- [51] N. Di Cesare, M. Belletête, F. Raymond, M. Leclerc, G. Durocher, *J. Phys. Chem. A* **1998**, *102*, 2700-2707.
- [52] M. Moreno Oliva, T. M. Pappenfus, J. H. Melby, K.M. Schwaderer, J.C. Johnson, K. A. McGee, D. A. da Silva Filho, J.L. Bredas, J. Casado, J. T. Lopez Navarrete, *Chem. Eur. J.* **2010**, *16*, 6866-6876.
- [53] F. Negri, M. Z. Zgierski, *J. Chem. Phys.* **1994**, *100*, 2571-2587.
- [54] P. Kölle, T. Schnappinger, R. de Vivie-Riedle, *Phys. Chem. Chem. Phys.* **2016**, *18*, 7903-7915.
- [55] R. Fitzner, E. Reinold, A. Mishra, E. Mena-Osteritz, H. Ziehlke, C. Körner, K. Leo, M. Riede, M. Weil, O. Tsaryova, A. Weiß, C. Urich, M. Pfeiffer, P. Bäuerle, *Adv. Funct. Mater.* **2011**, *21*, 897-910.
- [56] J. Min, Y.N. Luponosov, N. Gasparini, L. Xue, F.V. Drozdov, S.M. Peregudova, P.V. Dmitryakov, K.L. Gerasimov, D. V. Anokhin, Z.-G. Zhang, T. Ameri, S.N. Chvalun, D.A. Ivanov, Y. Li, S.A. Ponomarenkobi, C. J. Brabecaj, *J. Mater. Chem. A* **2015**, *3*, 22695-22707.

- [57] B. Dereka, A. Rosspeintner, Z. Li, R. Liska, E. Vauthey, *JACS* **2016**, *138*, 4643-4649.
- [58] B. Bardi, C. Dall'Agnes, K.I. Moineau-Chane Ching, A. Painelli, F. Terenziani, *J. Phys. Chem. C* **2017**, *121*, 17466-17478.
- [59] E. C. Taylor, D. E. Vogel, *J. Org. Chem.* **1985**, *50*, 1002-1004.
- [60] F. Parenti, P. Morvillo, E. Bobeico, R. Diana, M. Lanzi, C. Fontanesi, F. Tassinari, L. Schenetti, A. Mucci, *Eur. J. Org. Chem.* **2011**, 5659-5667.
- [61] Alex A. Granovsky, Firefly version 8.2.0, Available from: <http://classic.chem.msu.su/gran/firefly/index.html>.
- [62] M. W. Schmidt, K. K. Baldrige, J. A. Boatz, S. T. Elbert, M. S. Gordon, J. H. Jensen, S. Koseki, N. Matsunaga, K. A. Nguyen, S. Su, T. L. Windus, M. Dupuis, J. A. Montgomery, *J. Comput. Chem.* **1993**, *14*, 1347-1363.
- [63] M. Valiev, E.J. Bylaska, N. Govind, K. Kowalski, T.P. Straatsma, H.J.J. van Dam, D. Wang, J. Nieplocha, E. Apra, T.L. Windus, W.A. de Jong, *Comput. Phys. Commun.* **2010**, *181*, 1477-1489.
- [64] D.F. Eaton, *Pure & Appl. Chem.* **1988**, *60*, 1107-1114.
- [65] D. Magde, R. Wong, P. G. Seybold, *Photochem. Photobiol.* **2002**, *75*, 327-334.
- [66] S. J. Isak, E. M. Eyring, *J. Phys. Chem.* **1992**, *96*, 1738-1742.

TOC



Two A- -D- -A thiophene based small molecules with a central dithienosilole core and dicyanovinyl end groups were synthesized. Theoretical calculations, together with spectroscopic and electrochemical findings revealed that both molecules possess low band gaps, broad absorption spectra and a good stability both in p and n-doping states. The observed increasing of the electric dipole moment upon photoexcitation in such two quadrupolar-like molecules has been interpreted on the basis of the symmetry breaking in the S1 excited state.